SEA-LEVEL ANALYSIS USING 100 DAYS OF REFLECTED GNSS SIGNALS

Johan S. Löfgren, Rüdiger Haas, and Hans-Georg Scherneck

Department of Earth and Space Sciences, Chalmers University of Technology,
Onsala Space Observatory, SE-439 92 Onsala, Sweden
Email: johan.lofgren@chalmers.se, rudiger.haas@chalmers.se, and
hans-georg.scherneck@chalmers.se

ABSTRACT

Global Navigation Satellite System (GNSS) signals reflected off the sea surface can be used for remote sensing of the sea level. We present results from a GNSS-based tide gauge using standard geodetic-type GNSS receivers for receiving both the reflected and the direct GNSS signals. The local sea level is then obtained using relative geodetic processing of the carrier phase delay.

We show results from our analysis of 100 days of GNSS data from the Onsala Space Observatory (OSO). The GNSS-derived sea level is compared to a weighted average of sea level observations from two stilling well gauges located 18 km and 33 km away from OSO. The comparison shows a high level of agreement with a correlation coefficient of 0.96. Furthermore, the standard deviation (1σ) between the time series is 5.0 cm and the pairwise mean difference is 3.6 cm.

Additionally, we present a tidal analysis of the three sea level datasets and compare the derived tidal constituents both to each other and to a Regional Tide Model (RTM). From the GNSS-derived sea level we find significant ocean tidal signals with reasonable amplitudes and with most phases in between those for the stilling well gauges sites. The comparison to the RTM shows limitations of the model for long-period tidal signals.

Key words: GNSS; reflected signals; sea level.

1. INTRODUCTION

In 2009 *Löfgren et al.* [1] presented a new remote sensing technique for measuring local sea level using standard geodetic-type Global Navigation Satellite System (GNSS) receivers. This GNSS-based tide gauge uses both reflected GNSS signals from the sea surface and direct GNSS signals, similar to what was introduced by *Martin-Neira* [2]. However, instead of using an interferometric approach as, e.g., presented by *Rius et al.* [3], standard geodetic processing of the carrier phase delay measurements are used to derive estimates of sea level.

Traditional tide gauges provide sea-level measurements of the vertical distance between the sea surface and the land surface, i.e., measurements relative to the Earth's crust. This quantity is directly related to the volume of the ocean. However, in order to measure sea-level change due to ocean water volume and other oceanographic change, all types of land motion need to be known. If there are no available geodetic or geological dataset for the region, land motion corrections can not be applied, resulting in inaccurate inference of sea level at sites with major tectonic activity. Thus, these sites are often removed from the sea-level analysis, contributing to a geographical bias in the sea-level dataset [4].

Since GNSS can be used to measure land motion with respect to the Earth's centre of mass, the advantage of the GNSS-based tide gauge is that it can provide measurements of both sea surface height changes and land surface height changes. Furthermore, combining both measurements results in local sea level, which is automatically corrected for land motion. This means that the GNSS-based tide gauge can provide continuously reliable sea-level estimates in tectonic active regions.

The GNSS-based tide gauge was first deployed at the Onsala Space Observatory (OSO) on the west coast of Sweden at the end of 2008 showing promising sea level results [5]. Further campaigns have provided high-rate sea-level estimates [6] and in its current form, in which it has been operated since September 2010, provided long time series of local sea-level [7]. In this paper, we present results from the analysis of more than 100 days of GNSS data. The resulting sea-level estimates are compared to sea-level measurements from two stilling well gauges about 18 km south of and 33 km north of OSO. Furthermore, we present a tidal analysis of the three independent datasets.

2. THE GNSS-BASED TIDE GAUGE

The concept of the GNSS-based tide gauge builds upon bistatic radar measurements at L-band to estimate the local sea level. The installation consists of two antennas mounted back-to-back on a beam extending over

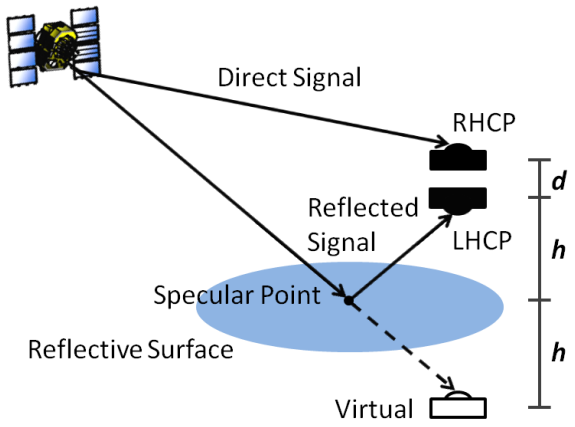

Figure 1. The concept of the GNSS-based tide gauge. The installation is receiving both direct GNSS signals, with the upward-looking right-hand circular polarized antenna, and GNSS signals reflected off the sea surface, with the downward-looking left-hand circular polarized antenna. Each antenna is connected to a standard geodetic-type GNSS receiver.

the coastline. Each antenna is connected to a standard geodetic-type receiver. The zenith-looking Right-Hand Circular Polarized (RHCP) antenna is tracking the direct GNSS signals, whereas the nadir-looking Left-Hand Circular Polarized (LHCP) antenna is tracking the reflected GNSS signals that have reflected of the sea surface, see Figure 1. After reflection off the sea surface the RHCP satellite signal becomes LHCP or actually left-hand elliptical polarized, see, e.g., *Löfgren et al.* [7].

With the additional travel time of the reflected signals, as compared to the directly received signals, the downward-looking antenna will appear to be a virtual (upward-looking) antenna located below the sea surface. The vertical distance below the sea surface of this virtual antenna h will be the same as the distance between the actual downward-looking antenna and the sea surface. This distance will change with changing sea surface and is directly proportional to the sea surface height. Moreover, from the geometry in Figure 1, h can be related to the vertical baseline between the two antennas Δv as $\Delta v = 2h + d$, where d is the vertical separation of the phase centres of the two antennas. By combining the RHCP measurement of land surface height with the LHCP measurement of sea surface height, local sea level can be obtained.

The current installation of the GNSS-based tide gauge at OSO extends about 1 m over the coastline with the downward-looking antenna about 1.2 m above mean sea level (local tidal range ∼20 cm). In order to maximize the number of sea surface reflections (visibility of satellites to the north is limited at these latitudes, 57° N) the installation is directed towards the south with open sea water in a southward direction from approximately azimuth 40° to 260°.

Data were collected during 107 days in 2010 from September 16 (00:00:00 UTC) to December 31 (23:59:59 UTC). The equipment used consisted of two Leica GRX1200 GNSS receivers, each connected to a Leica AR25 multi-GNSS choke-ring antenna (the downward-looking antenna was LHCP) protected by a hemispherical radome. Both receivers recorded continuous data with 1 Hz sampling during the entire campaign with the exception of a few shorter power failures.

3. DATA PROCESSING

The GNSS data were analyzed in post-processing using an in-house software for relative positioning developed in MATLAB. Global Positioning System (GPS) L_1 phase delays were used together with broadcast ephemerides [8] in standard geodetic processing using single differences according to

$$\lambda\Delta\Phi^j_{AB}(t) = \Delta\varrho^j_{AB}(t) - \lambda\Delta N^j_{AB} + c\Delta\tau_{AB}(t) \quad (1)$$

where λ is the wavelength of the GPS L_1 carrier, $\Delta\Phi^j_{AB}(t)$ are the measured carrier phase differences between the two receivers expressed in cycles, $\Delta\varrho^j_{AB}(t)$ are the differences in geometry, ΔN^j_{AB} are the phase ambiguity difference in cycles, c is the speed of light in vacuum, and $\Delta\tau_{AB}(t)$ are the receiver clock bias differences. The equation is expressed in meters and subscripts A and B denote the two receivers, superscript j denotes the satellite, and t denotes the epoch. Because of the short baseline, we assumed that both tropospheric and ionospheric effects are negligible. Furthermore, since the antennas were aligned horizontally, we only estimated the vertical baseline in the geometry term.

Before the processing an elevation and azimuth mask was applied to the data to remove unwanted observations from below 20° elevation and towards the northwest from 260° to 40° azimuth. The processing was done with a least-squares analysis for every 10 minutes using overlapping data intervals of 20 minutes for each solution. For every interval the software solved for vertical baseline (for the current interval), phase ambiguity differences (for each satellite pair), and receiver clock differences (for each epoch). For more information regarding the processing see *Löfgren et al.* [5, 7].

The vertical baseline solutions between the antennas were converted into a time series of local sea level using the previous mentioned equation (see Section 2). However, the vertical distance between the antenna phase centers where not accounted for, resulting in a bias. Furthermore, erroneous solutions were removed based the formal error in the least-squares minimization process (solutions with formal error of larger than 1 cm were disregarded) and outliers were removed based on a 4σ threshold from an averaged GNSS-derived time series created with a window size of 3.5 h (which removed in total 45 samples during the 107 days).

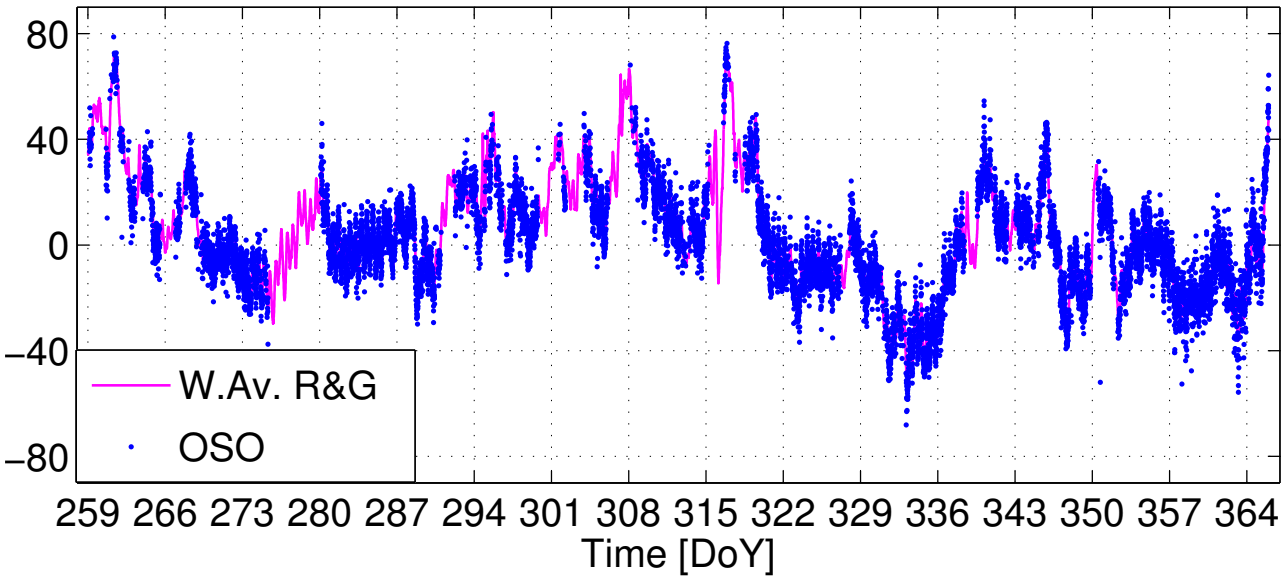

Figure 2. The GNSS-derived time series of sea level (blue dots) from Onsala Space Observatory (OSO) and the weighted average (W.Av. R&G) of the two stilling well gauge time series of sea level (magenta line) from Ringhals and Gothenburg. A mean is removed from each time series.

4. SEA-LEVEL ANALYSIS

The resulting GNSS-derived sea-level time series was compared to independent sea-level observations from two stilling well gauges operated by the Swedish Meteorological and Hydrological Institute (SMHI). These two stilling well gauges were situated about 18 km south (Ringhals) and 33 km north (Gothenburg) of OSO. The comparison was done both in the time domain and in the frequency domain as an ocean tide analysis.

4.1. Time Domain Comparison

Before the time domain comparison the more frequently sampled stilling well gauge time series were adjusted to the time tags of the GNSS-derived sea level, i.e., values every 10 minutes starting at the full hour. Furthermore, in order to compare the GNSS-derived time series to a more suitable reference, the stilling well gauge time series were combined into a weighted average time series. The weights were inversely proportional to the distance between the sites and OSO. The mean of each time series were then removed in order to avoid biases. Both the GNSS-derived sea level and the weighted average of the stilling well gauge sea level are shown in Figure 2 for Day-of-Year (DoY) 259 to 365.

First of all, it is clear from Figure 2 that the GNSS-derived sea level agrees well with the variations in the stilling well gauge sea level. Second, the GNSS-derived sea level is more noisy with possibly a few outliers left. Third, there are periods in the GNSS-derived time series where there are data gaps, e.g., DoY 276 to 280. These

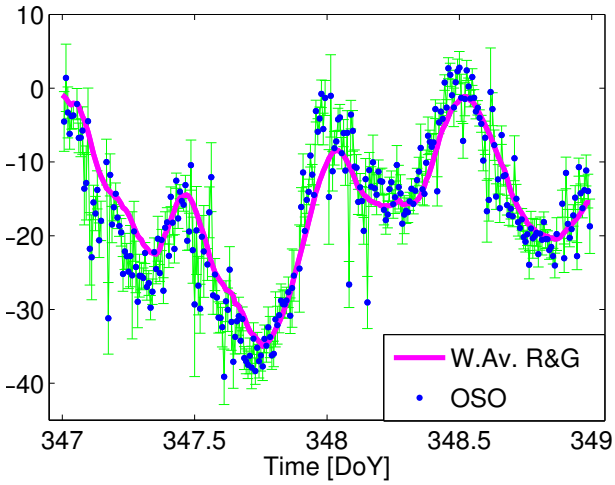

Figure 3. The GNSS-derived sea level (blue dots) with errorbars consisting of the formal errors in the least-squares minimization process times a factor of 10 (green vertical lines), and the weighted average stilling well gauge sea level (magenta line). A mean is removed from each time series.

data gaps are attributed to three factors: receiver power failure, software restrictions, and the receivers' capability of keeping lock on the reflected GNSS signals in high sea surface roughness, see [7].

Figure 3 depicts a zoom into Figure 2 during DoY 347 and 348, revealing finer features of the time series. Errorbars for the GNSS-derived sea level are shown in Figure 3, consisting of the formal errors in the least-squares

Table 1. Tidal components derived from tidal analysis of the GNSS-based tide gauge sea level and the stilling well gauge observations at Ringhals and Gothenburg together with tidal components from a Regional Tide Model (RTM). 107 days of data were used from the GNSS-based tide gauge, whereas one year of observations was used for the two stilling well gauges. Amplitudes are presented in millimeters and phases in degrees. The amplitude uncertainty (1σ) for the stilling well gauges are $\pm$ 0.1–0.4 mm, whereas the values for the GNSS-based tide gauge are shown in the table.

Tide	Site	RTM		Stilling well gauge		GNSS (Onsala)	
		Amplitude [mm]	Phase [°]	Amplitude [mm]	Phase [°]	Amplitude [mm]	Phase [°]
M_2	Onsala	58.5	156.6			66.4 ±8	155.2
	Ringhals	96.6	98.6	49.9	170.8		
	Gothenburg	59.7	147.7	73.0	125.1		
N_2	Onsala	6.4	174.2			11.9 ±9	85.4
	Ringhals	13.0	101.9	4.6	133.6		
	Gothenburg	6.4	161.5	16.5	70.8		
S_2+K_2	Onsala	12.4	123.4			15.0 ±8	87.7
	Ringhals	23.2	64.5	7.7	127.8		
	Gothenburg	13.4	114.0	13.3	82.5		
Q_1	Onsala	5.8	255.0			23.8 ±9	270.7
	Ringhals	3.9	110.9	5.3	289.7		
	Gothenburg	5.3	252.0	8.1	285.8		
O_1	Onsala	25.9	355.2			15.0 ±9	300.1
	Ringhals	4.9	312.6	17.2	307.0		
	Gothenburg	22.7	352.3	18.0	290.3		
M_f	Onsala	17.1	202.3			45.0 ±10	329.3
	Ringhals	16.8	201.9	20.8	97.4		
	Gothenburg	17.1	202.4	54.9	135.3		
M_m	Onsala	10.3	195.9			92.2 ±13	334.4
	Ringhals	10.3	200.2	113.5	316.6		
	Gothenburg	10.4	196.4	88.2	309.7		
M_4	Onsala	5.1	251.1			12.6 ±5	311.7
	Ringhals	6.3	192.8	5.1	337.1		
	Gothenburg	5.6	248.1	8.6	309.5		

minimization process times a factor of 10. It can be seen that also in detail there is a high level of agreement between the time series with the GNSS-derived sea level following the variations in the stilling well gauge sea level (correlation coefficient of 0.96). Additionally, the periodic signals (semi-diurnal) in Figure 3 suggests the impact of the local ocean tides at the sites.

The performance of the GNSS-based tide gauge is evaluated by using the weighted average sea level as the truth. From the difference between the sea level time series, the standard deviation (1σ) was calculated to 5.0 cm. Additionally, the pairwise mean and maximum differences were 3.6 cm and 28.5 cm, respectively. The GNSS-derived sea level is, as previously mentioned, more noisy than the stilling well gauge weighted average sea level. However, the high maximum difference is most probably due to an outlier which was not removed in the outlier editing.

4.2. Ocean Tide Analysis

An ocean tide analysis was performed for the GNSS-derived sea level time series and for both stilling well gauge sea level time series (Ringhals and Gothenburg). The harmonic parameters were computed on the basis of the *Tamura* [9] tide potential development. All available data (107 days) from the GNSS-based tide gauge were used and one full year of data (2010) from the stilling well gauges. Despite the more noisy time series, the GNSS-based tide gauge sea level permitted determination above 1σ for several major species with the following presented in Table 1: M_2, N_2, S_2+K_2, Q_1, O_1, M_f, M_m, and M_4.

In Table 1 we find that the GNSS-based tide gauge gives meaningful tide parameters for the analysed 107 days. Amplitudes are of reasonable magnitudes and most phases are in between those for the Ringhals and Gothenburg sites. Furthermore, we also compare the tide re-

sults with a Regional Tide Model (RTM) for Kattegat, see Table 1. The RTM is excited by TPXO.7.2 [10] with an addition of M_4 from FES2004 [11]. A comparison of the RTM results with those from the ocean tide analysis of the GNSS-derived sea level and the stilling well gauge sea level, shows quite good agreement for the semi-diurnal and diurnal tidal components. However, for the long period tidal components, there are large model deficiencies, with the exception of the amplitude of M_4. These deficiencies arise most probably due to weather driven long periodic variations, which are unmodeled. Furthermore, there are resonating features in Kattegat and the tide modeling is therefore highly sensitive to the conditions at the boundaries.

5. CONCLUSIONS AND OUTLOOK

The GNSS-based tide gauge at the Onsala Space Observatory (OSO) provides valuable sea level estimates that show good agreement with the weighted average of the independently observed sea-level data, from the two stilling well gauges at Ringhals and Gothenburg, with a correlation coefficient of 0.96. The GNSS-derived sea level is more noisy, with a few outliers, as compared to the stilling well gauge sea level. In a comparison the standard deviation (1σ) between the time series is 5.0 cm with a mean difference of 3.6 cm.

In the ocean tide analysis, several major tidal components were found in the GNSS-derived sea level. The harmonic parameters compared well with the amplitudes and phases from the analysis of the one year long data set from the stilling well gauges, which strengthens the usefulness of the GNSS-based tide gauge. Comparison to model calculations based on a region tide model reveals model limitations, in particular for the long period tidal components.

Currently, we are installing the GNSS-based tide gauge permanently at OSO. In addition, we are supplementing it with a pressure sensor tide gauge at the same site. This is done in order to further evaluate the GNSS-based tide gauge and to compare it to another technique with the same coastal geometry and hydrological conditions.

We are on our way to change the GNSS processing technique into double difference processing and plan to use a filter-based scheme, e.g., Kalman filter. Furthermore, we intend to add GLONASS (and in the future Galileo) observations in the processing to increase the number of solutions and improve the results.

ACKNOWLEDGMENTS

We would like to thank the Swedish Meteorological and Hydrological Institute for providing stilling well gauge data from the sites at Gothenburg and Ringhals. The equipment used for the GNSS-based tide gauge (receivers, antennas) were purchased via the Leica Geosystems ATHENA program. Finally, we would also like to thank Adlerbertska Forskningsstiftelsen for partially funding this project.

REFERENCES

[1] Löfgren J. S., Haas R., Johansson J. M., 2009, Sea Level Monitoring Using a GNSS-Based Tide Gauge, *Proc. 2nd Int. Coll. - Scientific and Fundamental Aspects of the Galileo Programme*, CD-ROM, ESA

[2] Martin-Neira M., 1993, A PAssive Reflectometry and Interferometry System (PARIS): Application to ocean altimetry, *ESA J.*, 17, 331–355

[3] Rius A., Nogués-Correig O., Ribó S., Cardellach E., Champs A., J. F. Marchán J. F., Valencia E., Rodríguez N., van der Marel H., Naeije M., M. Martin-Neira, 2009, PARIS interferometric technique: proof of concept, *Proc. 2nd Int. Coll. - Scientific and Fundamental Aspects of the Galileo Programme*, CD-ROM, ESA

[4] Bindoff N. L., Willebrand J., Artale V., Cazenave A., Gregory J., Gulev S., Hanawa K., Le Quéré C., Levitus S., Nojiri Y., Shum C. K., Talley L. D., Unnikrishnan A., 2007, Observations: Oceanic Climate Change and Sea Level, In: *Climate Change 2007: The Physical Science Basis*, Working Group I, 4th Assessment IPCC [Solomon S., Qin D., Manning M., Chen Z., Marquis M., Averyt K. B., Tignor M., Miller H. L. (eds.)], Cambridge University Press, Cambridge, United Kingdom and New York, NY, USA, 385–432

[5] Löfgren J. S., Haas R., Johansson J. M., 2011a, Monitoring coastal sea level using reflected GNSS signals, *J. Adv. Space Res.*, *47(2)*, 213–220

[6] Löfgren J. S., Haas R., Johansson J. M., 2010, High-rate local sea level monitoring with a GNSS-based tide gauge, *Proc. 2010 IEEE International Geoscience and Remote Sensing Symposium*, 3616–3619

[7] Löfgren J. S., Haas R., Scherneck H.-G., Bos M. S., 2011a, Three months of local sea level derived from reflected GNSS signals, *Radio Sci.*, doi:10.1029/2011RS004693

[8] Dow J. M., Neilan R. E., Rizos C., 2009, The International GNSS Service in a changing landscape of Global Navigation Satellite Systems, *J. Geod., 83*, 191–198

[9] Tamura Y., 1987, A harmonic development of the tide- generating potential, *Bull. Info. Maries Terrestres*, *99*, 6813–6855

[10] Egbert G. D., Erofeeva S. Y., 2002, Efficient inverse modeling of barotropic ocean tides, *J. Atmos. Oceanic Technol.*, *19*, 183–204

[11] Letellier T., 2004, *Etude des ondes de mare sur les plateux continentaux*, Ph.D. Thesis, Université de Toulouse III, Ecole Doctorale des Sciences de l'Univers, de l'Environnement et de l'Espace, Toulouse, France